

## Supporting Information File

### **Small Molecule Interactions with Biomacromolecules: Selective Sensing of Human Serum Albumin by a hexanuclear manganese complex: photophysical and biological studies**

Rousunara Khatun,<sup>a,b</sup> Malay Dolai,<sup>c</sup> Mihir Sasmal,<sup>a</sup> Atul Katarkar,<sup>d</sup> Abu Saleh Musha Islam,<sup>e</sup> Nasima Yasmin\*,<sup>b</sup> Sana Maryum<sup>a</sup>, Jebiti Haribabu,<sup>f,g</sup> Mahammad Ali,<sup>\*a</sup>

<sup>a</sup> Department of Chemistry, Jadavpur University, 188, Raja S. C. Mullick Road, Kolkata 700 032, India. *E-mail:* *m\_aliz062@yahoo.com*.

<sup>b</sup> Aliah University, II-A/27, Action Area II, Newtown, Action Area II, Kolkata, West Bengal 700160, India.

<sup>c</sup> Department of Chemistry, Prabhat Kumar College, Purba Medinipur 721404, India

<sup>d</sup> Department of Biochemistry, University of Lausanne, 1066 Epalinges, Switzerland.

<sup>e</sup> School of Chemical Sciences, Indian Association for the Cultivation of Science, & 2B Raja S.C. Mullick Road, Kolkata 700032, India.

<sup>f</sup> Facultad de Medicina, Universidad de Atacama, Los Carreras 1579, 1532502 Copiapo, Chile.

<sup>g</sup> Chennai Institute of Technology (CIT), Chennai 600069, India.

#### **Instrumentation:**

The Fourier transform infrared (FT-IR) spectra in the range 450–4000 cm<sup>-1</sup> on KBr pellets was recorded using an IR 750 series-II FT-IR (Nicolet Magna) spectrophotometer. The UV-Vis spectra were recorded on an Agilent diode array spectrophotometer (Model Agilent 8543). The fluorescence spectra were recorded at room temperature in a PTI spectrofluorimeter (Model QM-40) with fluorescence-free quartz cuvette of 1 cm path length. The excitation and emission slit widths were fixed at 3 nm. The electrospray ionization mass spectra ESI-MS<sup>+</sup> (m/z) were produced on a High-Resolution Mass Spectrometer (Model: QTOF Micro YA263). Single crystal X-ray diffraction data were accumulated using a Bruker SMART APEX II Diffractometer using monochromated MoK<sub>α</sub> radiation (λ = 0.71073 Å). Fluorescence lifetimes were determined from time-resolved intensity decay by the method of time correlated single photon counting (TCSPC) measurements using a picosecond diode laser (IBH Nanoled-07) in an IBH fluorocube apparatus. The fluorescence decay data were collected on a Hamamatsu MCP photomultiplier (R3809) and examined by the IBH DAS6 software. Circular dichroism (CD) spectral investigations were performed in a PC-driven JASCO J815 (Japan) spectropolarimeter. The Origin Lab Software version 8.5 was used to analyze the experimental results and statistical evaluation.

#### **UV-Vis and fluorescence studies**

All the UV-Vis spectra were collected with proper background correction. The absorption titrations were carried out under two conditions: (i) concentration of HSA was kept fixed at 5 μM while the concentration of **1** was varied between 0 and 15 μM; (ii) concentration of **1** was kept fixed at 5 μM while the concentration of HSA was varied between 0 and 25 μM. Likewise, fluorescence titrations were also carried out under two conditions: (i) upon excitation at 300 nm, HSA (0-15 μM) was gradual added into the of 5 μM solution of complex **1** in Tris–HCl buffer; and (ii) upon excitation at 295 nm, complex **1** (0-15 μM) was gradual added into the of 5 μM solution of HSA in Tris–HCl buffer.

The inner filter effect correction has been carried out for all the fluorescence spectra gave in the manuscript according to the following equation:<sup>S1</sup>

$$I = I_{obs} \times e^{(A_{ex} + A_{em})/2} \quad (Eq. S1)$$

Here, the corrected and observed emission intensity are denoted by  $I$  and  $I_{obs}$ , correspondingly.  $A_{ex}$  and  $A_{em}$  denotes the absorbance value of the sample at the excitation and emission wavelengths, respectively. In the fluorescence selectivity experiment, the test samples were prepared by adding the appropriate amounts of the stock solutions of the respective proteins and enzymes into 5  $\mu$ M solution of complex **1**. For the competitive fluorescence displacement experiments, stock solutions of warfarin and ibuprofen (1 mM for each) were prepared in deionized water and DMSO, respectively. Here, also stock solution of hemin site marker ( $1 \times 10^{-3}$  M) was prepared in DMSO solution. In a typical assay, HSA solution was premixed with complex **1** at a molar ratio 1:4. Then, this mixed solution was further spiked with different amounts of warfarin/ibuprofen/hemin and the resultant ternary mixtures were subjected to fluorescence measurement. In case of another fluorescence site marker displacement assay, HSA solution was premixed with site markers (warfarin, ibuprofen and hemin) at a molar ratio 1:1 and then complex **1** was gradually added from 0 to 15  $\mu$ M.

### Fluorescence lifetime measurements

The TCSPC measurements were carried out in 10 mM Tris-HCl buffer solution of pH 7.4 for the fluorescence decay of complex **1** in the absence and in the presence of increasing concentration of HSA at 298 K. Further, the fluorescence decay of HSA was performed in the absence and in the presence of increasing concentration of complex **1** to assess the interaction between HSA and complex **1**. The instrument response function (IRF) was ascertained experimentally by using dilute micellar solution of SDS in water as light signal scatterer. During the TCSPC measurements the photoexcitation was fixed at 300 nm for both HSA and complex **1**. The fluorescence decay curves were fitted to a biexponential function:

$$I(t) = A + \alpha_1 \cdot e^{(-t/\tau_1)} + \alpha_2 \cdot e^{(-t/\tau_2)} \quad (Eq. S2)$$

Where,  $\alpha_i$  represents the  $i$ th pre-exponential factor and  $\tau_i$  denotes the decay time of component  $i$  (here  $i = 1, 2$ ). The average lifetimes ( $\tau_{avg}$ ) for the fluorescence decay profiles were calculated by using the following equation:<sup>S2</sup>

$$\tau_{avg} = \sum_{i=1}^2 \alpha_i \cdot \tau_i / \alpha_i \quad (Eq.S3)$$

### Circular dichroism (CD) spectra

All the reported CD spectra were recorded in the wavelength range 195-300 nm under constant purging of nitrogen and a scan speed of 100 nm  $\text{min}^{-1}$ . Here, a fixed concentration of HSA (5  $\mu$ M) was titrated with the increasing concentration of complex **1** from 0  $\mu$ M to 15  $\mu$ M in Tris-HCl buffer solution of pH 7.4 at 298 K. Each CD spectrum was an average of five scans and the baseline correction was performed with Tris-HCl buffer signal.

### **Esterase-like activity study**

The esterase-like activity study was performed to determine the effect of complex **1** on the functionality of HSA. Here, the HSA activity is examined by measuring the absorbance value of *p*-nitrophenol ( $\lambda_{\text{abs}} = 400 \text{ nm}$ , molar extinction coefficient,  $\epsilon = 17,700 \text{ M}^{-1} \text{ cm}^{-1}$ )<sup>S3-S5</sup> as formed by the reaction between the substrate (*p*-nitrophenyl acetate (PNPA)) and the enzyme (HSA). The reaction kinetics was recorded on Agilent 8453 UV-Vis Spectrophotometer. Here, the reaction conditions were maintained as follows: [HSA] = 5  $\mu\text{M}$ , [PNPA] = 10  $\mu\text{M}$ , pH 7.4, temperature = 37 °C. Here, one unit of activity is expressed as to be the quantity of HSA required for releasing 1  $\mu\text{M}$  *p*-nitrophenol per minute at 37 °C.

### **Cell culture and cytotoxicity assay**

A549 (Adenocarcinomic human alveolar basal epithelial cells) and Wi38 (human fetal lung fibroblast cells) cells were cultured in complete media containing Dulbecco's Modified Eagle Medium (DMEM) + 10% Fetal bovine serum (FBS) complemented with antibiotics (penicillin-100  $\mu\text{g}/\text{ml}$ ; streptomycin-50  $\mu\text{g}/\text{ml}$ ) at 37°C in 95% air, 5% CO<sub>2</sub> incubator.  $5 \times 10^3$  cells per well were placed in 96 well plates, the cells were incubated at different concentrations of complex **1** for an additional 24 h. Next, 10  $\mu\text{L}$  MTT solution (10 mg/ml PBS) was added to each well of a 96-well culture plate and again incubated continuously at 37 °C for a period of 3h. The relative cell viability, incubated with complex **1** and a control for untreated cells, was determined by measuring the MTSformazan absorbance on a microplate reader at 490 nm (Tecan, Infinite 200 PRO, Switzerland).

### **Cell Imaging study by fluorescence microscope**

A549 cells were seeded on cover slip in 35x10 mm culture dish for 24 h at incubator. A549 cells were incubated without/with HSA (5 and 10  $\mu\text{M}$ ) in serum free DMEM media for 4 h. Cells were washed with 1X PBS buffer (pH 7.4) for three times. Subsequently, cells were treated with 10  $\mu\text{M}$  complex **1** for 30 min in serum free DMEM media. Next, the cells were washed with PBS buffer (pH 7.4) and mount on coverslips. Bright field and fluorescence images of A549 cells were taken by fluorescence microscope (Leica DM3000, Germany) with an objective lens of 40X magnification.

### **Colony formation assay**

The cytotoxicity effects of complex **1** were confirmed further by colony formation assay on A549 cell line which was performed according to our previously standardized protocol. Briefly Cells were seeded in a 6 well plate at a low density (500 cells in 2 ml/well) and were treated with two different doses of Complex **1** (10  $\mu\text{M}$  and 20  $\mu\text{M}$ ) and incubated for 5 days. Colony numbers were counted after fixing and staining the cells with crystal violet solution (Gram's crystal violet, Merck). All the statistical analysis was performed using GraphPad Prism 8.0.

### **Sphere assay**

Multicellular 3D tumour spheroid model was performed using A549 cells in a liquid overlay method following a previously described method.<sup>S6</sup> Cells were seeded at 3000-5000 cells/ml in 35 mm plates pre-coated with 1% agarose (wt/volume) and incubated with 5% humidified CO<sub>2</sub> incubator and regularly checked for spheroid formation. After spheroid formation, cells were treated with the two selected doses of complex **1** and the change in the morphology and size were noted upto 7 days. Images were taken in bright field in an inverted microscope (Olympus). All the statistical analysis was

performed using GraphPad Prism 8.0. The spheres size measured as perimeter ( $\mu\text{m}$ ) on digitally acquired images by Image J software (<https://imagej.net/ij/>).

### Molecular docking study

To determine the plausible binding site within HSA and the mode of binding of complex **1** with HSA, molecular docking studies was carried out using docking program AutoDock (version 4.2). The X-ray crystal structure of HSA was obtained from the RCSB Protein Data Bank with the PDB ID: 2bxh. Alongside, the crystal structure of complex **1** was used for the Auto Dock 4.2 programs. Gasteiger charges and polar hydrogen atoms were added to the HSA and complex **1**. Using the AutoGrid tool, a grid box with dimensions of  $120 \text{ \AA} \times 120 \text{ \AA} \times 120 \text{ \AA}$  and  $0.403 \text{ \AA}$  grid spacing were selected to accommodate the protein. The Lamarckian genetic algorithm (LGA) was used to accomplish the docking calculations.<sup>57,58</sup> The docking outcome results were analyzed and visualized by using Discovery Studio and PyMOL soft wares.

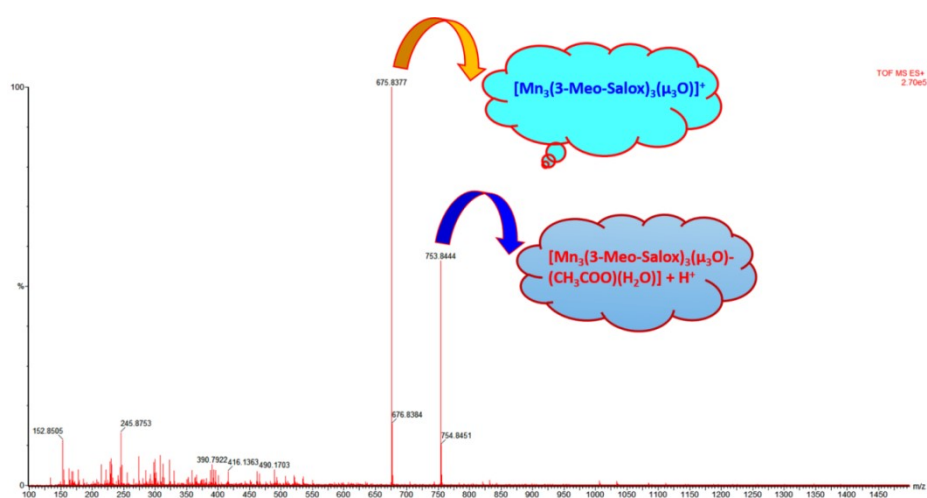


**Figure S1.** ESI-MS<sup>+</sup> (m/z) spectrum denotes full spectrum of complex **1** in MeCN.

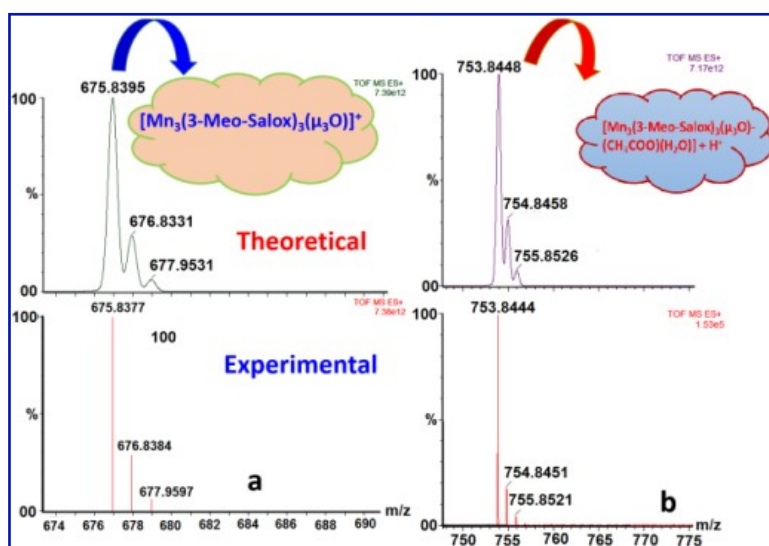


**Figure S2.** ESI-MS<sup>+</sup> (m/z) spectrum denotes simulated spectrum of  $[\text{Mn}_3(\mu_3\text{-O})(3\text{-MeO-salox})_3]^+$   $[\text{Mn}_3(\mu_3\text{-O})(3\text{-MeO-salox})_3(\text{OAc})(\text{H}_2\text{O})] + \text{H}^+$  in MeCN.

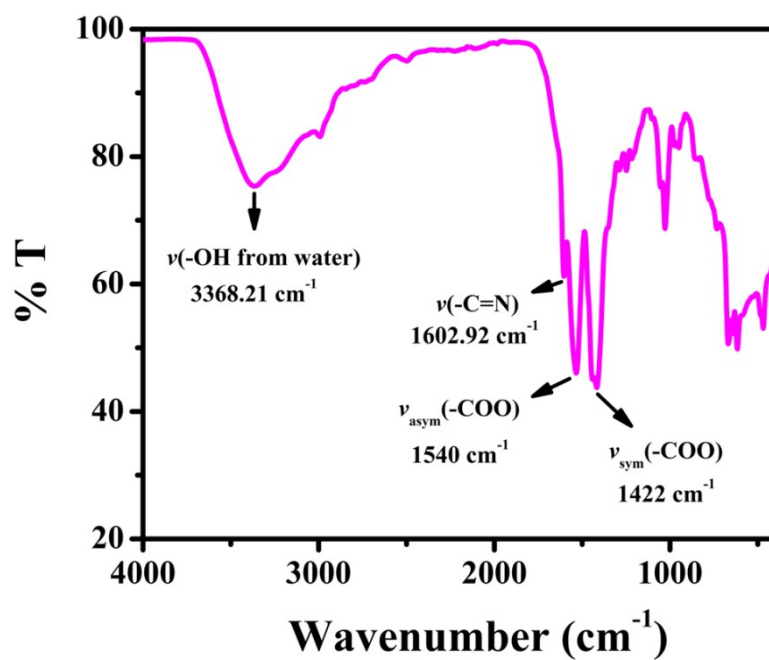


Figure S3. FT-IR spectrum of complex 1.

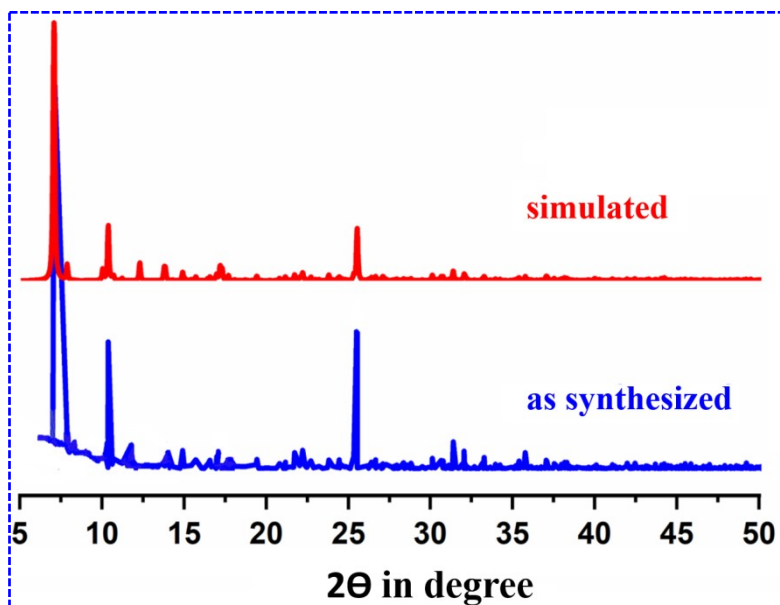
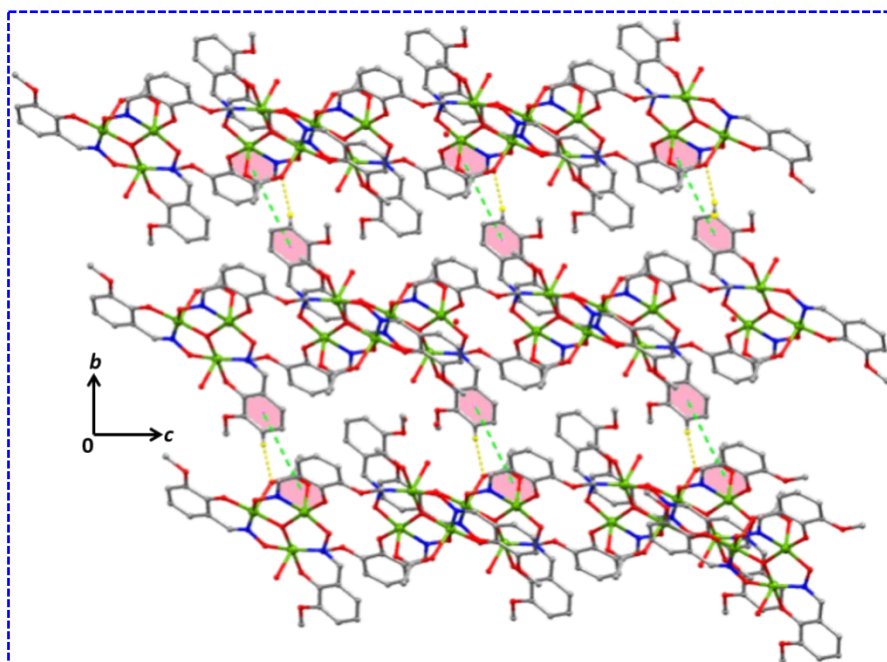
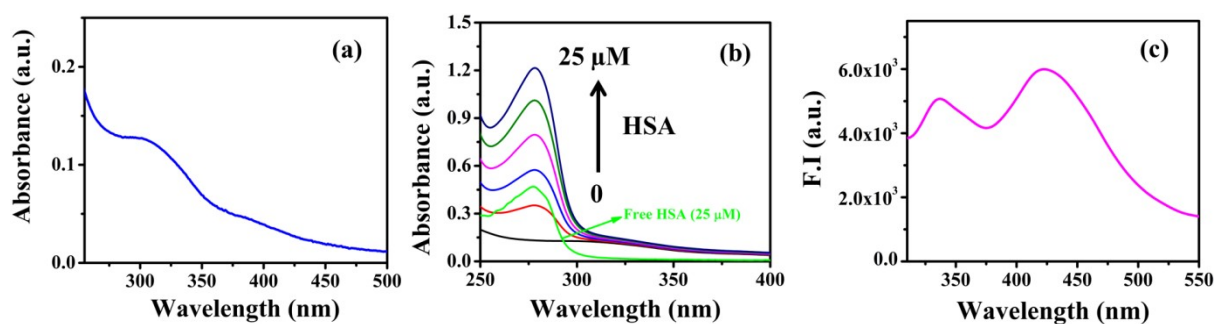


Figure S4. Synthesized (blue) and simulated (Red) X-ray powder diffraction pattern of complex 1.



**Figure S5.** The H-bonded 2D network in crystallographic *bc* plane in complex **1**.



**Figure S6.** (a) Absorption spectra of complex **1** ( $5 \mu\text{M}$ ). (b) Absorption titration of complex **1** ( $5 \mu\text{M}$ ) with the incremental addition of HSA (0- $25 \mu\text{M}$ ). (c) Fluorescence emission spectra of complex **1** ( $5 \mu\text{M}$ ) in Tris-HCl buffer (pH 7.4),  $\lambda_{\text{ex}} = 300 \text{ nm}$ .

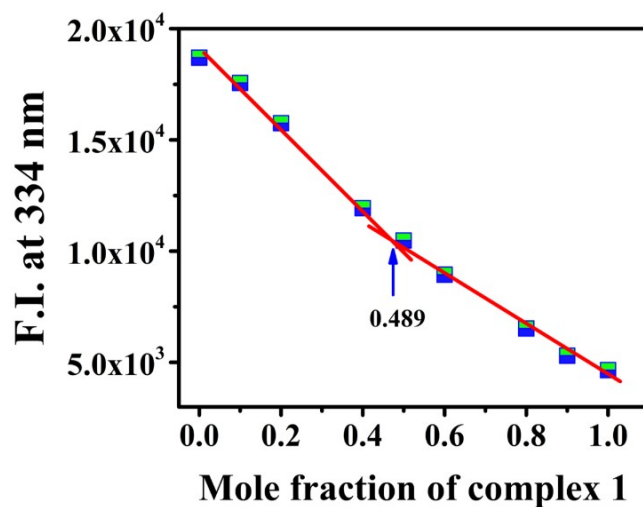


**Figure S7.** Job's plot for the binding of complex **1** with HSA.

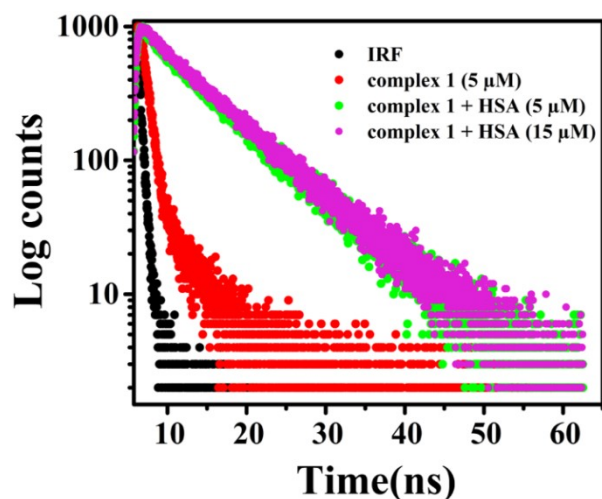


**Figure S8.** Representative time-resolved fluorescence decay spectra of complex 1 (5  $\mu\text{M}$ ) in the absence and with the incremental addition of HSA (0–15  $\mu\text{M}$ ).

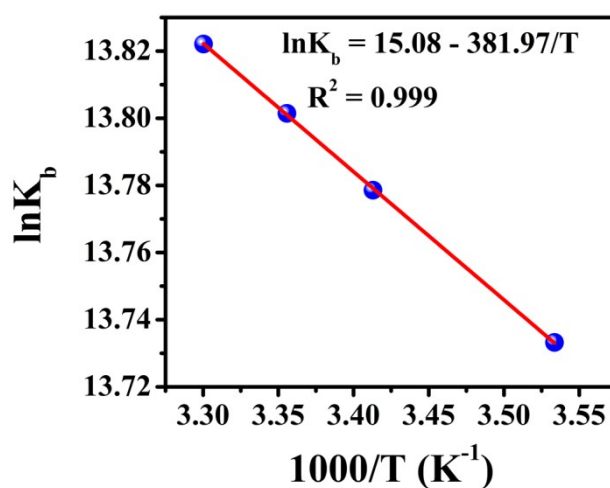


**Figure S9.** Van't Hoff plot for complex 1 and HSA association.

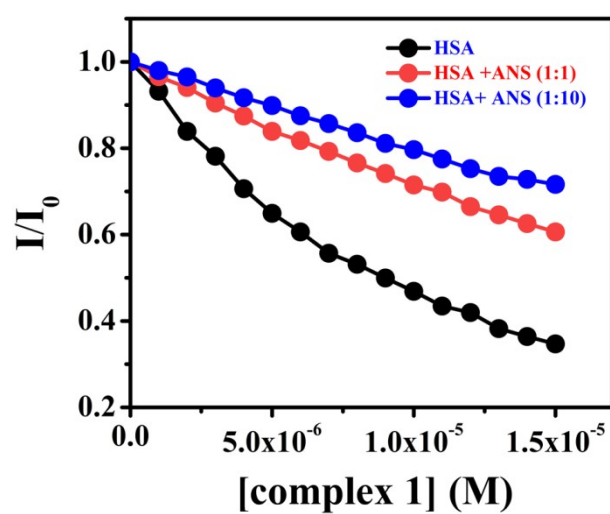


**Figure S10.** ANS displacement experiment for the fluorescence quenching of HSA:ANS composite at different ratios (1:0, 1:1 and 1:10) with the gradual addition of complex 1.

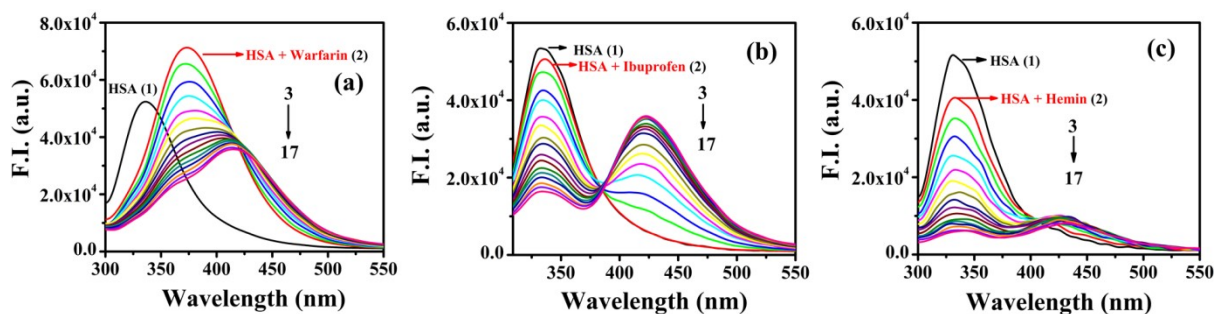


**Figure S11.** Effect of complex **1** on the emission of HSA–site marker composites. (a) [HSA] = [warfarin] = 5  $\mu\text{M}$ , (b) [HSA] = [ibuprofen] = 5  $\mu\text{M}$  and (c) [HSA] = [hemin] = 5  $\mu\text{M}$ . For all the panel (a), (b) and (c) curves 3-17 represent the addition of complex **1** each time 1  $\mu\text{M}$  to a total 15  $\mu\text{M}$  concentration.  $\lambda_{\text{ex}} = 295 \text{ nm}$ .

**Table S1.** Crystal data and details of refinement for complex **1**.

CCDC	2345419
Formula	$\text{C}_{52} \text{H}_{48} \text{Mn}_6 \text{N}_6 \text{O}_{28}, 4(\text{O})$
Formula Weight	1598.60
Crystal System	Triclinic
Space group	$P\bar{1}(\text{No. } 2)$
a, b, c [ $\text{\AA}$ ]	11.344(18) 12.359(17) 12.444(18)
$\alpha, \beta, \gamma$ [ $^\circ$ ]	67.20(3) 86.85(4) 88.90(4)
V [ $\text{\AA}^3$ ]	1606(4)
Z	1
D(calc) [ $\text{g}/\text{cm}^3$ ]	1.653
$\mu(\text{MoK}\alpha)$ [ $\text{mm}^{-1}$ ]	1.240
F(000)	808
Crystal Size [mm]	0.09 x 0.18 x 0.25
Temperature (K)	298
Radiation [ $\text{\AA}$ ]	$\text{MoK}\alpha$ 0.71073
Theta Min-Max [ $^\circ$ ]	2.5, 27.1
Dataset	-13: 13; -14: 14; -14: 13
Tot., Uniq. Data, R(int)	10264, 7118, 0.136
Observed data [ $ I  > 2.0 \text{ sigma}(I)$ ]	1973
R, $wR_2(\text{reflections})$	0.063(1973), 0.1847 (7118)



**Table S2.** Selected bond distances and angles (Å) in complex 1.

Bond	Bond Distances (Å)	Bond	Bond Angles (Å)
Mn1–O4	1.892	O4–Mn1–O5	175.3(4)
Mn1–OA	1.943(11)	O4–Mn1–O6	89.3(3)
Mn1–O5	1.870	O4–Mn1–OA	89.7(4)
Mn1–O6	2.157(9)	O4–Mn1–NJ	90.2(4)
Mn1–NJ	1.984(13)	O4–Mn1–OAa	84.2(3)
Mn1–OA	2.521(10)	O6–Mn1–OA	96.5(4)
Mn2–O4	1.878(9)	O6–Mn1–NJ	98.2(4)
Mn2–O7	1.865(10)	O5–Mn1–OAa	91.2(3)
Mn2–O9	2.117(11)	O6–Mn1–OA	96.5(4)
Mn2–OC	1.916(10)	O6–Mn1–NJ	98.2(4)
Mn2–NH	2.029(11)	O6–Mn1–OAa	172.3(4)
Mn3–O1	2.656(19)	OA–Mn1–NJ	165.3(4)
Mn3–O4	1.861(9)	OA–Mn1–OAa	79.5(3)
Mn3–O8	1.848(10)	OAa–Mn1–NJ	85.9(4)
Mn3–OB	2.342(11)	O4–Mn2–O7	170.1(4)
Mn3–OD	1.883(11)	O4–Mn2–O9	91.2(4)
Mn3–NI	1.992(12)	O4–Mn2–OC	92.2(4)
		O4–Mn2–NH	89.3(4)
		O7–Mn2–O9	98.6(4)
		O7–Mn2–OC	86.8(4)
		O7–Mn2–NH	89.0(4)
		O9–Mn2–OC	103.4(4)
		O9–Mn2–NH	92.6(4)
		OC–Mn2–NH	163.9(5)
		O1–Mn3–O4	90.4(4)
		O1–Mn3–O8	90.4(5)
		O1–Mn3–OB	164.3(4)
		Mn01–O4–Mn03	120.3(5)
		Mn02–O4–Mn03	120.6(4)

**Table S3.** Time-resolved fluorescence decay parameters of complex **1** (5  $\mu\text{M}$ ) with the gradual addition of HSA at 298 K.

System	[HSA] ( $\mu\text{M}$ )	$\tau_1$ (ns)	$\alpha_1$ (%)	$\tau_2$ (ns)	$\alpha_2$ (%)	$\langle\tau\rangle$ (ns)	$\chi^2$
complex 1-HSA	0	0.67	89.04	4.79	10.96	1.12	0.945
complex 1-HSA	5	1.87	5.86	8.05	94.14	7.69	0.988
complex 1-HSA	15	1.90	5.13	8.09	94.87	7.71	1.021

**Table S4.** Time-resolved fluorescence decay parameters of HSA (5  $\mu\text{M}$ ) with the gradual addition of complex **1** at 298 K.

System	[complex 1] ( $\mu\text{M}$ )	$\tau_1$ (ns)	$\alpha_1$ (%)	$\tau_2$ (ns)	$\alpha_2$ (%)	$\langle\tau\rangle$ (ns)	$\chi^2$
HSA-complex1	0	1.755	20.81	6.354	79.19	5.40	1.066
HSA-complex1	2	1.769	23.65	6.274	76.35	5.21	1.031
HSA-complex 1	4	1.792	24.75	6.243	75.25	5.14	1.020
HSA-complex 1	7	1.834	28.66	6.124	71.34	4.89	1.011
HSA-complex 1	10	1.855	32.57	6.039	67.43	4.67	1.010
HSA-complex 1	13	1.868	37.04	5.981	62.96	4.45	0.989
HSA-complex 1	15	1.879	37.74	5.995	62.26	4.44	1.001

## References

- S1) C. Jash, P. V. Payghan, N. Ghoshal and G. S. Kumar, *J. Phys, Chem. B*, 2014, **118**, 13077-13091.
- S2) B. Ojha and G. Das, *J. Phys. Chem. B*, 2010, **114**, 3979–3986.
- S3) H. Ostdal and H. Andersen, *Food Chem.*, 1996, **55**, 55-61.
- S4) G. Rabbani, M. H. Baig, E. J. Lee, W.K. Cho, J. Y. Ma and I. Choi, *Mol. Pharmaceutics*, 2017, **14**, 1656-1665.
- S5) G. Rabbani, E. J. Lee, K. Ahmad, M. H. Baig and I. Choi, *Mol. Pharmaceutics*, 2018, **15**, 1445-1456.
- S6) R. Khatun, R. Modak, A. S. M. Islam, D. Moni, N. Sepay, R. Mukherjee, G. Das, N. Murmu and M. Ali, *ACS Appl. Bio Mater.*, 2023, **6**, 3176–3188.
- S7) G. M. Morris, D. S. Goodsell, R. Huey and A. J. Olson, *J. Comput. Aided Mol. Des.*, 1996, **10**, 293–304.
- S8) G. M. Morris, D. S. Goodsell, R. S. Halliday, R. Huey, W. E. Hart, R. K. Belew and A. J. Olson, *J. Comput. Chem.*, 1998, **19**, 1639–1662.